# Wind energy

Karl Nilsson
Stefan Ivanell

Gotland University
*Passion & Science*

Wind energy

Typeset in $\mathcal{AMS}$-LaTeX

*Front cover illustration shows a wind resource map of Hunnflen located in Dalarna, Sweden.*

# Contents

# Nomenclature and glossary

$N = kg\frac{m}{s^2}$ - Definition of the unit N (Newton) in SI units.

| Roman letters | Description | Dimension | Value |
|---|---|---|---|
| $a$ | Axial interference factor | $-$ | $-$ |
| $a_{acc}$ | Acceleration | $m/s^2$ | $-$ |
| $A, B$ | Stability coefficients | $-$ | $-$ |
| $A_c$ | Cross section area | $m^2$ | $-$ |
| $A_{weibull}$ | Weibull scale factor | $m/s$ | $-$ |
| $c_1, c_2, c_\mu$ | Constants | $-$ | $-$ |
| $c_p$ | Heat capacity of air | $Nm/K$ | $-$ |
| $C_p$ | Efficiency of wind turbine | $-$ | $-$ |
| $C_{p,max}$ | Betz' limit | $-$ | $16/27$ |
| $C_T$ | Thrust coefficient | $-$ | $-$ |
| $E_\infty$ | Energy content in free stream air | $Nm$ | $-$ |
| $E_{kin}$ | Kinetic energy, $P_{kin}t$ | $Nm$ | $-$ |
| $E_o$ | Energy content in air behind rotor | $Nm$ | $-$ |
| $E_r$ | Energy content in air at rotor | $Nm$ | $-$ |
| $f$ | Coriolis parameter | $rad/s$ | $-$ |
| $F_c$ | Coriolis force | $N$ | $-$ |
| $F_{cent}$ | Centrifugal force | $N$ | $-$ |
| $F_f$ | Friction force | $N$ | $-$ |
| $F_g$ | Gravitational force | $N$ | $-$ |
| $F_p$ | Pressure gradient force | $N$ | $-$ |
| $g$ | Gravitational constant | $m/s^2$ | $9,82$ |
| $h, z, z_a$ | Heights | $m$ | $-$ |
| $H_0$ | Heat flux | $N/ms$ | $-$ |
| $k$ | Turbulent kinetic energy | $Nm$ | $-$ |
| $k_{weibull}$ | Weibull k shape factor | $-$ | $-$ |
| $L$ | Monin-Obukhov length | $m$ | $-$ |
| $m$ | Mass | $kg$ | $-$ |
| $\dot{m}$ | Massflow of air | $kg/s$ | $-$ |
| $\dot{m}_\infty$ | Massflow of free stream air | $kg/s$ | $-$ |
| $\dot{m}_o$ | Massflow of air behind rotor | $kg/s$ | $-$ |
| $\dot{m}_w$ | Massflow of in in wake | $kg/s$ | $-$ |
| $p$ | Pressure | $N/m^2$ | $-$ |
| $P_\eta$ | Porosity | $-$ | $-$ |
| $P_{kin}$ | Kinetic power | $Nm/s$ | $-$ |

| | | | |
|---|---|---|---|
| $P_{max}$ | Maximum power in streaming air | $Nm/s$ | − |
| $P_r$ | Output power of turbine | $Nm/s$ | − |
| $r$ | Radius | $m$ | − |
| $r_w$ | Radius of wake | $m$ | − |
| $r_o$ | Radius of air wake behind rotor | $m$ | − |
| $t$ | Time | $s$ | − |
| $T, \Delta F$ | Thrust force | $N$ | − |
| $T_0$ | Absolute temperature | $K$ | − |
| $u, u', u''$ | Wind velocities | $m/s$ | − |
| $u_*, u_{*1}, u_{*2}$ | Friction velocities | $m/s$ | − |
| $u_\infty$ | Free stream air velocity | $m/s$ | − |
| $u_o$ | Air velocity behind rotor | $m/s$ | − |
| $u_r$ | Air velocity at rotor | $m/s$ | − |
| $u_w$ | Air velocity in wake | $m/s$ | − |
| $\delta u$ | Velocity decifit | − | − |
| $x$ | Directional variable | $m$ | − |
| $z_0, z_{01}, z_{02}$ | Roughness lengths | $m$ | − |

| Greek letters | Description | Dimension | Value |
|---|---|---|---|
| $\alpha$ | Wake expansion coefficient | − | − |
| $\varepsilon$ | Turbulent dissipation rate | $Nm/(kgs)$ | − |
| $\kappa$ | von Karman's constant | − | 0,40 |
| $\nu$ | Kinetic viscosity | $m^2/s$ | − |
| $\nu_T$ | Turbulent viscosity | $m^2/s$ | − |
| $\rho$ | Density of air | $kg/m^3$ | 1,225 |
| $\varphi$ | The latitude | $\circ$ | − |
| $\omega$ | Earth's angular rotation speed | $rad/s$ | |

| Glossary | Description |
|---|---|
| $AEP$ | Annual Energy Production |
| $CFD$ | Computational Fluid Dynamics |
| $DK$ | Digitala Kartbiblioteket |
| $m.a.s.l.$ | Meters above sea level |
| $Orography$ | Height variation |
| $WAsP$ | Wind Atlas Analysis and Application Program for wind energy simulations |
| $WindPRO$ | Wind Atlas software |
| $WindSim$ | Wind energy simulation software |

# Chapter 1

# Wind energy

When estimating wind energy production one must keep in mind that the used model is barely a simplification of the reality. There are no "answers" regarding the energy production, why the reliability of the estimation software is important.

Wind energy conversion is a highly complex area in which a large number of parameters are involved. Energy estimation through various models is therefore also highly complex. For instance, the roughness classification is probably the most subjective part of the simulation process and is therefore a source of uncertainty whether thouroghly analyzed or not. By focusing on the roughness classification this uncertainty can however be minimized. The data, such as wind data and terrain data, used in the simulations does also pose uncertainties on the results. For instance, wind data is only valid for the measurement period and normally, the user wants to predict the energy production at a future site. This can only be done by using data from the past, why there are always inaccuracies in the resuts.

This chapter presents how winds are approximated, measured, visualized and converted into electricity. It also presents two limitations of wind energy conversion, i.e., Betz' limit, which states that no more than 16/27 of the wind energy can be converted into electrical energy, and wind wakes, which is described in the wind wake section.

## 1.1   Approximations of winds

The air in the atmosphere is affected by various forces which are due to gravitation, rotation of the earth, sun radiation, ground friction and the movement of the air. Wind, i.e., moving air, is therefore dependent on these forces. This section will start by stating and explaining these forces and end

with putting these forces together in horizontal and vertical balances, [1].

### 1.1.1   Forces affecting wind

If we consider a small air parcel, there are different forces causing the parcel to move and thus creating wind. These forces will be described in this subsection.

**Gravitational force**   The air parcel has a certain mass, $m$. This mass in combination with the gravitational constant, $g$ defines the gravitational force according to equation 1.1. The force is directed downwards. Figure 1.1 presents the gravitational force.
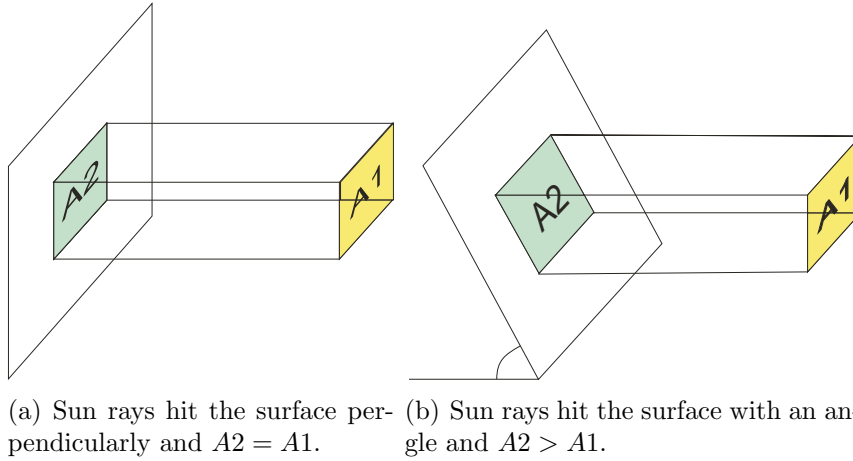
$$F_g = mg \tag{1.1}$$
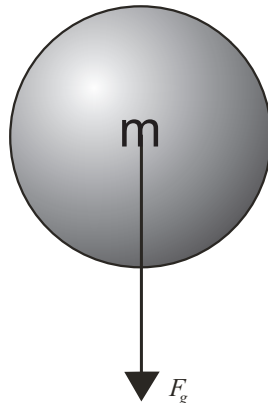


**Figure 1.1:** The circle represents an air parcel with mass m and the black arrow represents the gravitational force directed towards the ground.

**Pressure gradient force**   Since earth orbits the sun and in the same time rotates around its axis the sun radiation will not be equally distributed over the surface of the earth. The temperature will therefore differ around the globe since it is dependent on the energy per square meter due to sun radiation which in turn is dependent on the angle of which the sun rays hit the earth. For instant, if the sun rays hit the earth surface perpendicularly,

the area where a certain amount of sun energy hits the surface is small in comparison, making the sun energy per square meter high and also the temperature. If the same amount of sun energy hits the surface but with a certain angle, the energy will be smeared on a larger area and the sun energy per square meter will be low and thus leading to a low temperature, as shown in figure 1.2. Furthermore, the air in the atmosphere will therefore have different temperatures. When the air parcels are heated, they expand and high pressure areas are created. The high pressure air seeks equilibrium and moves towards low pressure areas. The pressure gradient force is a result of the pressure differences.



(a) Sun rays hit the surface per- (b) Sun rays hit the surface with an an-
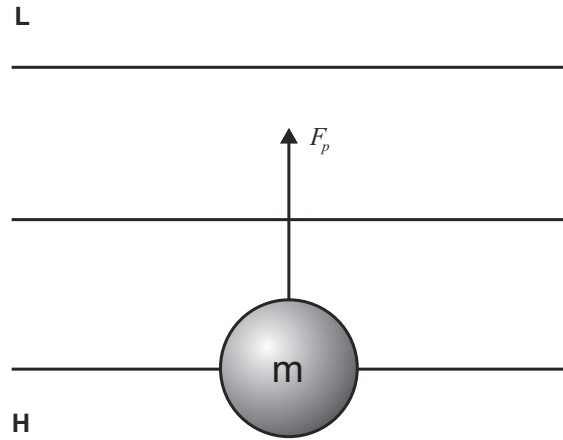pendicularly and $A2 = A1$.        gle and $A2 > A1$.

**Figure 1.2:** Sun ray smearing due to difference in hit angle.

The pressure gradient force is defined according to equation 1.2.

$$F_p = -\frac{m}{\rho}\frac{\partial p}{\partial n}$$
(1.2)

where $p$ is pressure, $n$ is the normal to the isobars, and $\rho$ the air density. The pressure gradient force is presented in figure 1.3.

3

**L**



**H**

**Figure 1.3:** The circle represents an air parcel and the black arrow represents the pressure gradient force directed towards the low pressure area, L.

**Coriolis force**   The Coriolis force is due to the earth's rotation and will cause the high pressure winds to move clockwise on the northern hemisphere and low pressure winds will move counter clockwise. The contrary applies for the southern hemisphere.

The Coriolis force is defined according to equation 1.3.

$$F_c = \pm f u \tag{1.3}$$

where $u$ is the wind speed and $f = 2\omega \sin(\varphi)$. $\omega$ is the angular speed of the earth's rotation and $\varphi$ is the latitude.
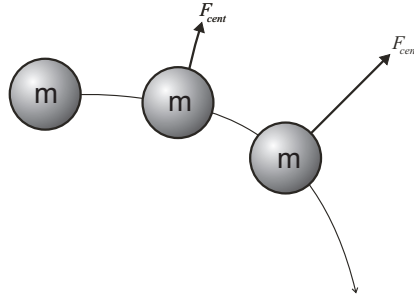
**Centrifugal force**   When the air parcel suddenly change direction of movement it is affected by a force directed perpendiculary to the change of direction, as shown in figure 1.4.

This force is named centrifugal force is defined according to equation 1.4.

$$F_{cent} = m \frac{u^2}{r} \tag{1.4}$$

where $r$ is the radius of the direction change.

**Friction force**   When air sweeps over the ground, friction appears. This friction in turn leads to a friction force directed in opposite direction to the wind direction. The friction force is dependent on wind speed and the

**Figure 1.4:** The circles represents an air parcel at different locations on its trajectory, the black arrow represents the centrifugal force affecting the air parcel.

so called roughness length which basically is a measure of how much the ground surface retards the wind speed at a certain location. A high roughness length retards the wind speed more than a low roughness length. Therefore, the friction force is higher in areas with high roughness length, e.g. dense forests, than in areas with low roughness length, e.g. open water. Roughness lengths are most often used in its classified version; the roughness class. The relationship between roughness length and class is presented in table 1.1. Figure 1.5 displays the friction force.

The friction force is defined according to equation 1.5.

$$F_f = -ku \tag{1.5}$$

where $k = f(z_0)$ and $z_0$ is the roughness length which is defined according to equation 1.6.

$$z_0 = ze^{-\frac{\kappa u}{u_*}} \tag{1.6}$$

where $z$ is the height, $\kappa$ is von Karmans constant and $u_*$ is the friction velocity.

## 1.1.2  Putting forces together

The wind is moving in a three dimensional pattern. This pattern is influenced by the forces described above. The forces in turn exist either in the vertical direction or in the horizontal plane. The vertical direction and the horizontal plane accounts for the three dimensional space in where the wind moves. This section aims at identifying vertical and horizontal forces, respectively, and to balance these. This section is alsp providing the hydrostatic balance in the vertical direction and three different balances for the horizontal plane.
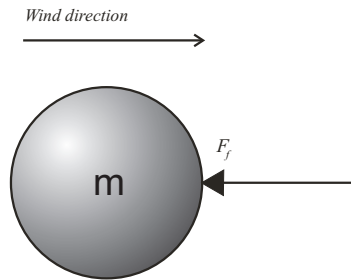
**Figure 1.5:** The circle represents an air parcel and the black arrow represents the friction force

| Roughness class | Roughness length [m] | Type of landscape |
|---|---|---|
| 0 | $\leq$ 0,0002 | Open water |
| 1 | 0,003 | Open landscape |
| 2 | 0,10 | Partly open landscape |
| 3 | 0,40 | Smaller cities |
| 4 | 1,60 | Large cities or dense forests |

**Table 1.1:** Relationship between roughness class, roughness length and landscape type

**Hydrostatic balance**   There are mainly two forces acting on the air parcel in the vertical direction; the gravitational force and the vertical pressure gradient force. Therefore, these forces are equal at static equilibrium state which is called hydrostatic balance. In this case the air parcel is static why the centrifugal force, which is due to movements of the parcel, is disregarded. Equation 1.7 defines the hydrostatic balance.

$$F_g = F_p \tag{1.7}$$

**Geostrophic balance**   The geostrophic balance is a good approximation of wind direction and speed at a high altitude, normally at a height of 1000 m, [18]. This balance is used by both WAsP and WindSim as inputs in order to describe winds at high altitudes. An air parcel is influenced by two forces according to the geostrophic balance; the coriolis force and the pressure gradient force. The pressure gradient force is always directed towards low pressure, and thus perpendicular to the isobars. The coriolis force is directed so that the wind moves clockwise according to figure 1.6. The so called geostrophic wind occurs when the the pressure gradient force and the coriolis

force are equal. The wind is then traveling parallel to the isobars. The geostrophic wind is also unaffected by the friction of the ground, [1].
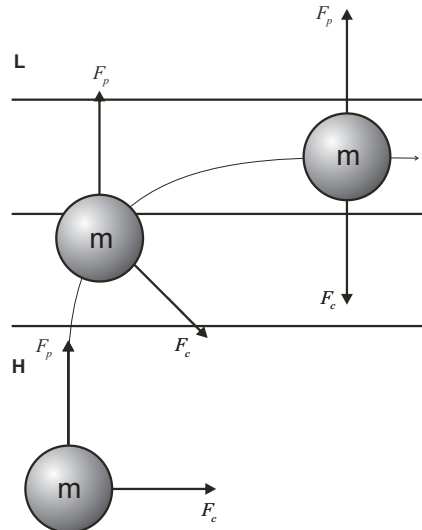


**Figure 1.6:** When the pressure gradient force is equal to the coriolis force, the geostrophic balance, the air will travel parallel to the isobars.

**Gradient balance**   The geostrophic balance requires that the wind blows in a straight line without change of direction. If this is not the case, as in most cases, the effects of the centrifugal force have to be taken into account. The centrifugal force will always be directed perpendicular to the change of direction as presented in figure 1.4.

**Guldberg-Mohn balance**   The Guldberg-Mohn balance applies for conditions close to the earth's surface. This approximation is a revision of the geostrophic balance as it adds the friction force to the balance. The friction force will be in opposed direction to the wind and will therefore slow the wind down. This will in turn make the coriolis force smaller since it is dependent on the wind speed. This results in a decreased wind speed and furthermore that the wind will cross the isobars with a certain angle, which is determined by the strength of the friction force and thus the roughness length of the surface, as the coriolis force is weakened.

**The logarithmic velocity profile**   The logarithmic velocity profile is basically an approximation of the vertical wind profile and is described by the

logarithmic velocity law, equation 1.8. Figure 1.7 shows the velocity log profile.

$$u = \frac{u_*}{\kappa} ln \frac{z}{z_0} \tag{1.8}$$
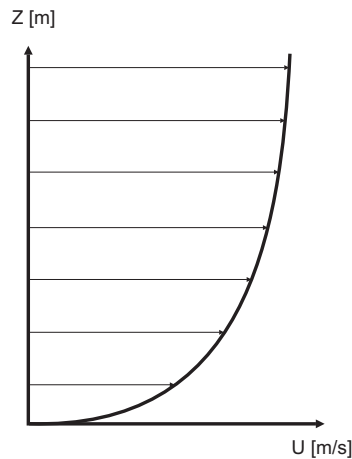


**Figure 1.7:** The logarithmic velocity profile.

## 1.2   Atmospheric stability

Atmospheric stability determines how well the atmosphere resists vertical movement of air parcels and is defined with the environmental lapse rate, where lapse rate is defined as the rate of temperature decrease due to increased elevation, and the so called adiabatic rate. The adiabatic rate is the rate at which the air parcel cools and compresses or heats and decompresses without interchanging heat with the surroundings. The dry adiabatic rate applies for unsaturated air and is more or less constant at 10 K cooling or warming per 1000 meter of change in elevation (cooling applies for increase in elevation and vice verse). The moist adiabatic rate applies for saturated air, when the air has a relative humidity of 100%. This rate is always lower than the dry adiabatic rate and is not constant as it varies with e.g. temperature, [2][4].

### 1.2.1 Absolute stable atmosphere

The atmosphere is absolute stable when the environmental lapse rate is lower than the moist adiabatic rate. For instance, if an air parcel in a stable atmosphere is elevated it will be cooled faster than the surroundings since its adiabatic cooling rate is higher than the environmental lapse rate. The air parcel will therefore be heavier than the surroundings and sink back to equilibrium state. The opposite applies when the air parcel is lowered. In this case the adiabatic heating rate is higher than the environmental lapse rate and thus resulting in that the air parcel is lighter than the surroundings. The air parcel will in this case rise back to equilibrium state, [2][4].

### 1.2.2 Neutral stable atmosphere

When the environmental lapse rate is equal to either the dry adiabatic rate at unsaturated conditions or the moist adiabatic rate at saturated conditions the atmosphere is neutral stable. This basically means that the air parcel will be heated or cooled with the same rate as its surroundings and thus have the same weight. The air parcel will in this case neither rise nor sink after perturbation, [2].

### 1.2.3 Absolute unstable atmosphere

The atmosphere is absolute unstable when the environmental lapse rate is higher than the dry adiabatic rate. In this case an elevated air parcel cools slower than the environmental lapse rate and is therefore warmer, and lighter, than the surroundings. It rises until an unstable equilibrium state is reached. A lowered air parcel continues sinking until unstable equilibrium is reached, [2][4].

### 1.2.4 Conditional stable atmosphere

When the environmental lapse rate lies between the dry and moist adiabatic rate, the atmosphere is conditionally stable. This means that when air is unsaturated the atmosphere is stable and when air is saturated the atmosphere is unstable, [2].

### 1.2.5 Variation over time

The atmospheric stability varies over time and is never constant at a certain location. At a site located on-shore the stability varies according to a 24

hour cycle, with a stable atmosphere during the night and a more unstable atmosphere during the day as shown in figure 1.8. The same cycle applies for off-shore conditions but is in this case over a longer period of time, which could be weeks or even months and is due to fact that water can "store" more energy than the ground, [11].
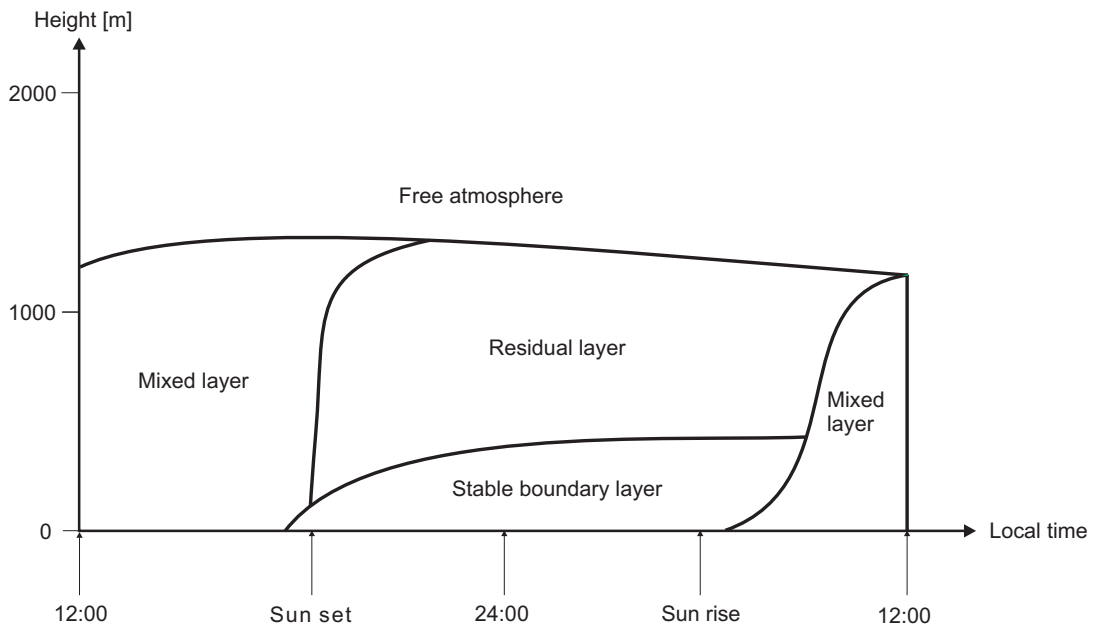
**Figure 1.8:** Changes of meteorological boundary layer during the day, [11].

## 1.3   Handling of wind data

In order to determine the wind conditions at a specific site one can measure the wind conditions directly on site or make a wind atlas calculation in order to transfer wind data from one site to another. This section describes different techniques in how to measure wind conditions. It describes how to calculate wind atlas data and it provides different ways of displaying wind energy content.

### 1.3.1   Measurement

The most accurate way of obtaining wind data is to simpy put a measuring device on the site. Measuring wind conditions on site gives you the possibility

to register wind speeds and wind directions at different heights. These data can later be used to determine frequency distribution of the wind, energy content in the wind and the distribution of the wind direction. The result becomes more accurate if the measuring takes place during a long period of time, [18]. Various techniques can be used for measuring wind data, such as traditional anemometers and more modern SODARs and LIDARs which are using sound and light, respectively, in the measurement.

## 1.3.2 Transfer

Measuring wind conditions is very time consuming. The so called wind atlas method offers a way to convert nearby located measuring points' data to the desired location, [18]. At location A a measuring mast has been collecting wind data for a satisfying period of time hence accurate profiles of wind frequency, direction and energy content have been established. The next step is to convert the measured data into wind atlas data. The wind data is dependent to the roughness class at the site. The data is recalculated to suit a roughness class of 1. This data is called the wind atlas data. The roughness class is determined at location B. The wind atlas data is again recalculated from roughness class 1 to the current roughness class of location B. Site B must be situated in a close radius to site A to get reliable results. Figure 1.9 shows the scheme of the wind atlas method.
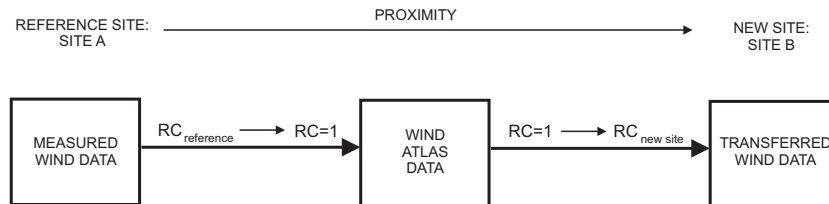


**Figure 1.9:** Wind atlas method.

## 1.3.3 Visualization

By using the wind atlas method, wind resource maps can be created, [18]. These maps give a rough view on how winds are distributed over land and sea. In Sweden, there are two types of wind resource maps; those who are displaying mean wind speed and those who are displaying energy content per square meter. The relationship between mean wind speed and energy content per square meter is shown in equations 1.9 to 1.14.

Equation 1.9 describes the kinetic power in the wind.

$$P_{kin} = \frac{1}{2}\dot{m}u^2 \tag{1.9}$$

The massflow of wind is described according to equation 1.10.

$$\dot{m} = \rho A_c u \tag{1.10}$$

Equation 1.9 and 1.10 give,

$$P_{kin} = \frac{1}{2}\rho A_c u^3 \tag{1.11}$$

The energy in the wind is given according to equation 1.12 where the time is converted from seconds to hours by dividing $t$ with 3600.

$$E_{kin} = P_{kin}t = \frac{1}{2}\rho A_c u^3 \frac{t}{3600} \tag{1.12}$$

In the next step the energy in the wind is converted in energy per square meter according to equation 1.13.

$$e_{kin} = \frac{E_{kin}}{A_c} = \frac{1}{2}\rho u^3 t \tag{1.13}$$

Number of hours per year, 8760, inserted in 1.13 give 1.14.

$$e_{kin,year} = \frac{1}{2}\rho u^3 8760 \tag{1.14}$$

where $P_{kin}$ is the power, $\dot{m}$ the massflow of air, $u$ is mean wind speed, $\rho$ is the density of air at a certain altitude, $A_c$ is cross section area, $E_{kin}$ is energy, $e_{kin}$ is energy per square meter and $t$ is the time. Figure 1.10 presents a wind resource map.
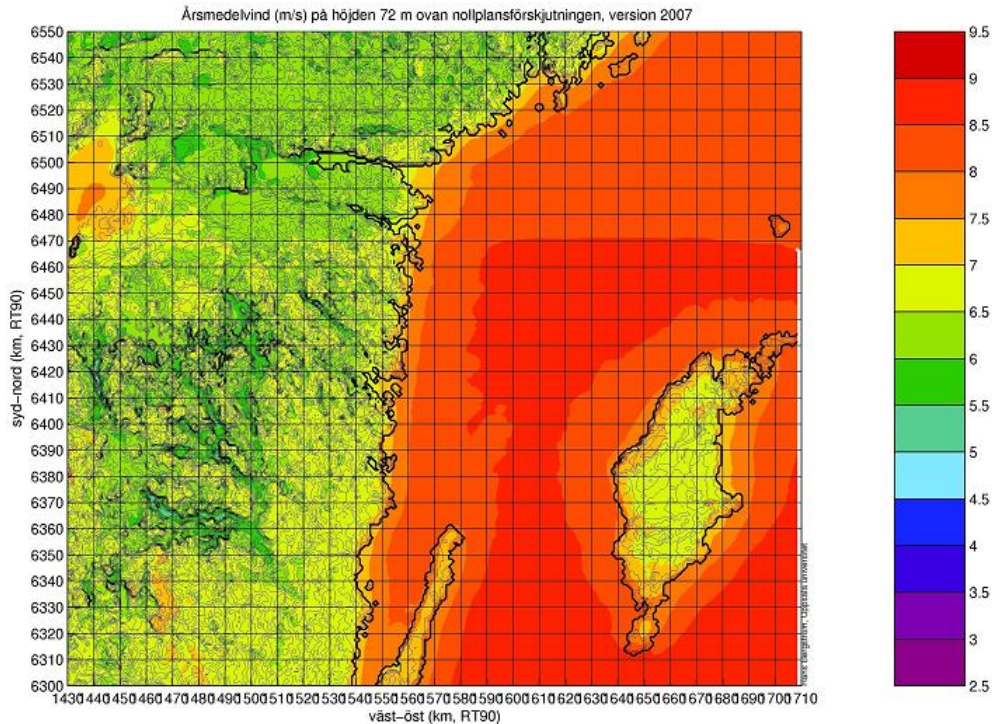
**Figure 1.10:** A wind resource map displaying mean wind speed over a part of Sweden, [3].

## 1.4 Conversion

The energy in the wind is converted into electricity by a wind turbine. In this section a typical wind turbine will be described briefly in terms of type of wind turbine and power control. These aspects affect the efficiency of the turbine aswell as the power curve.

### 1.4.1 Power control

There are two different ways of controlling the power output of the wind turbine; pitch and stall regulation.

In order to decrease the power output with a pitch regulated turbine the blades pitches out of the wind in order to reduce the lift force and the rotation speed and thus the power output.

In the case of stall regulation, there are again two types; passive and active stall. In the case of passive stall, the rotor blades are bolted in a fix angle. When the wind speed reaches a certain amount, the momentum

around the blades increases and the lift power decreases and so does the power output.

In the case of active stall, the rotor blades pitches into the wind in order to decrease the lift force and thus the power output, [13].

Figure 1.11 shows how the power curves vary for a wind turbine with passive stall regulation, NEG Micon 52, and a turbine with pitch regulation, Vestas V52.
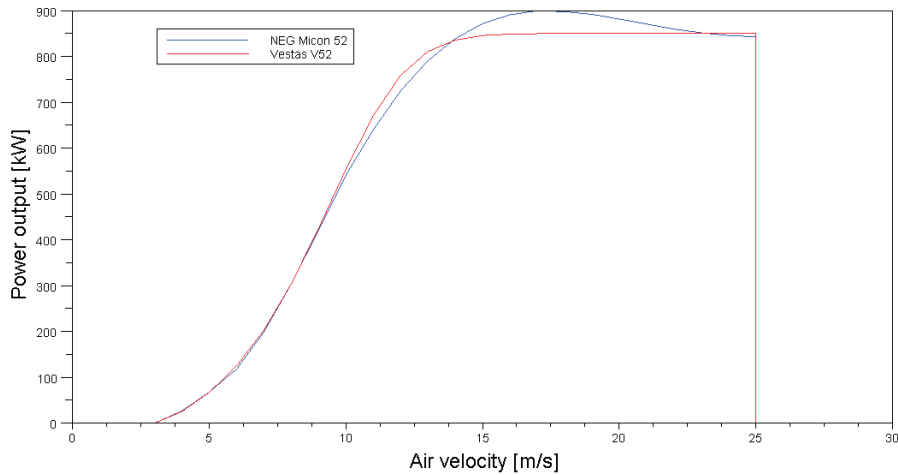


**Figure 1.11:** Stall and pitch power regulated wind turbines.

## 1.5 Betz' limit

A wind turbine can never have an efficiency of 100% even when disregarding from operational losses. As shown below, the efficiency of the wind turbine can never exceed 16/27 or roughly 59% and this is called the Betz' limit, [7][18].

The first step when determining the Betz' limit is to make an energy balance over the control volume shown in figure 1.12 and thus declaring the energy over the rotor, as decribed by equation 1.15.

$$E_\infty = E_r + E_o \implies E_r = E_\infty - E_o \tag{1.15}$$
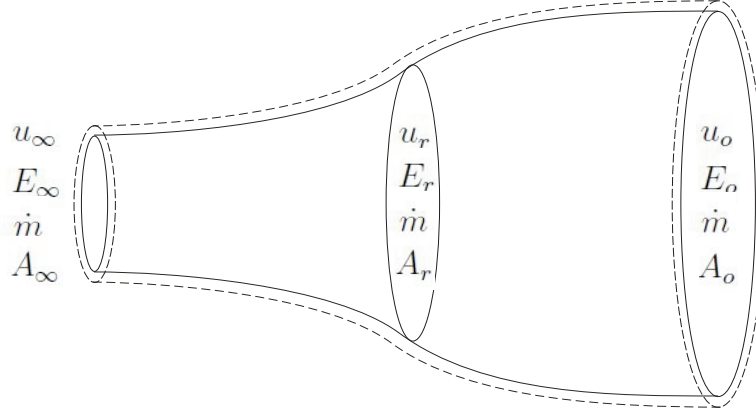
**Figure 1.12:** Control volume, [7].

Where $E$ is energy, $\infty$ stands for free stream air, $r$ stands for rotor and $o$ stands for out, i.e., perturbed air going out from the turbine.

Furthermore, the massflow is equal throughout the control volume, as described by equation 1.16.

$$\dot{m} = (\rho A_c u)_\infty = (\rho A_c u)_r = (\rho A_c u)_o \tag{1.16}$$

where $A_{c,\infty}$, $A_{c,r}$ and $A_{c,o}$ are cross sections areas shown in figure 1.12.

$u_r$ can be calculated by using two different formulas describing the power over the rotor. First, the power is described by making a balance of forces around the rotor, as described by equation 1.17.

$$dF = dma_{acc} = dm\frac{du}{dt} = \dot{m}du \implies \Delta F = \dot{m}\Delta u \tag{1.17}$$

where $dF$ is force acting on the air parcel with the weight $dm$. $a_{acc}$ is the acceleration of the air parcel and $\Delta F$ is the change of force which is equal to the trust force $T$ according to 1.18.

$$\Delta F = T \tag{1.18}$$

The deficit of air velocity is equal to the difference between the velocity at the inlet and the velocity at the outlet according to equation 1.19.

$$\Delta u = (u_\infty - u_o) \tag{1.19}$$

Equation 1.17, 1.18, 1.19 and the redefined $T$ give,

$$T = \dot{m}(u_\infty - u_o) \tag{1.20}$$

The output power of the turbine is defined in equation 1.21.

$$P_r = \frac{dE_r}{dt} = \frac{T dx}{dt} = T u_r \tag{1.21}$$

Equation 1.16, 1.20 and 1.21 give

$$P_r = (\rho A_c u^2)_r (u_\infty - u_o) \tag{1.22}$$

The same power can be described by using kinetic energy, $E = \frac{1}{2} m u^2$ and equation 1.15 give,

$$E_r = \tfrac{1}{2} m (u_\infty^2 - u_o^2)$$

using the differential equation according to equation 1.23 gives,

$$\implies dE_r = \frac{1}{2} dm (u_\infty^2 - u_o^2) \tag{1.23}$$

Equation 1.21 and 1.23 give,

$$P_r = \tfrac{dE_r}{dt} = \tfrac{1}{2} dm (u_\infty^2 - u_o^2) \tfrac{1}{dt} =$$

$$= \frac{1}{2} \dot{m} (u_\infty^2 - u_o^2) = \frac{1}{2} (\rho A_c u)_r (u_\infty^2 - u_o^2) \tag{1.24}$$

Equation 1.22 equals equation 1.24 which gives equation 1.25,

$$(\rho A_c u^2)_r (u_\infty - u_o) = \frac{1}{2} (\rho A_c u)_r (u_\infty^2 - u_o^2) \tag{1.25}$$

In which $u_r$ can be determined as a function of $u_\infty$ and $u_o$

$$u_r = \frac{1}{2} (u_\infty + u_o) \tag{1.26}$$

At this stage parameter $a$ is introduced. $a$ is the axial interference factor and is a measure of the air velocity decifit over the turbine.

$$a = \frac{u_\infty - u_r}{u_\infty} \tag{1.27}$$

Equation 1.27 gives,

$$u_r = u_\infty(1 - a) \tag{1.28}$$

Equation 1.26 and 1.28 give,

$$u_o = u_\infty(1 - 2a) \tag{1.29}$$

Equation 1.24, 1.28 and 1.29 give,

$$P_r = \frac{1}{2}(\rho A_c)_r u_\infty^3 [4a(1 - a)^2] \tag{1.30}$$

$$P_{max} = \frac{1}{2}(\rho A_c)_r u_\infty^3 \tag{1.31}$$

Equation 1.30 and 1.31 give,

$$C_p = \frac{P_r}{P_{max}} = 4a(1 - a)^2 \tag{1.32}$$

To calculate a maximum of $C_p$ for a certain $a$ one put $\frac{dC_p}{da} = 0$ $C_{p_{max}} = \frac{16}{27}$ for $a = \frac{1}{3}$ and this is called Betz' limit.

Betz' limit states that the efficiency of a single wind turbine can never exceed approximately 59%. This is hereby defined as the aerodynamic efficiency. In operation, there are also other types of losses in a wind turbine, e.g. friction losses which will reduce the turbine efficiency further, [18].

## 1.6 Wind wakes

When determining Betz' limit one stated that a wind turbine can only use about 59% of the wind energy. This is achieved when the free stream air velocity is retarded with 2/3. The free stream air velocity behind the turbine is therefore only 1/3 of the velocity in front the turbine. Since the wind energy is dependent of the wind velocity, the wind contains less energy after the turbine than in front of. This phenomenon is referred to as wind wakes and when wakes from many turbines interact it is called wind wake interaction. To minimize the effect of wind wake interaction, turbines are normally placed in a certain pattern in relation to the predominant wind direction. The wind wake interaction will decrease the production of wind farms depending on the size of the farm. For a farm of 5-10 turbines a decrease of approximately 5% in production can be expected, [18]. Figure 1.13 shows a model of a wake after a wind turbine.
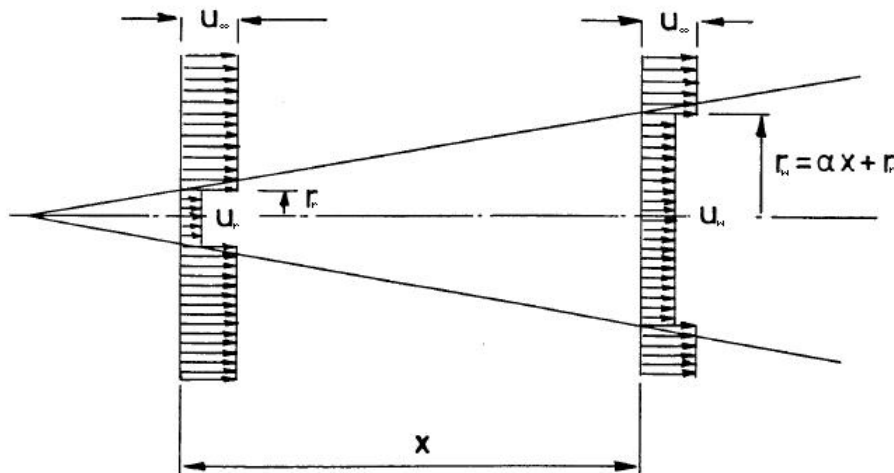


**Figure 1.13:** Principle scetch over the linear wake expansion according to N.O. Jensen, [8].

Wind wakes are however not only developed after wind turbines. There are also wind wakes after obstacles such as trees and houses. All wakes are characterized by turbulence, i.e., fast fluctuations of wind speed and direction, and are dependent on the size of the obstacle and porosity of such, [18].

# Chapter 2

# Software

In this chapter WindPRO, WAsP and WindSim are presented in general terms.

## 2.1 WindPRO

WindPRO is a software used for designing and planning for single wind turbines and wind farms. The software has been developed for more than 20 years by EMD International A/S in Aalborg, Denmark. The software has a modular structure which means that only the needed modules have to be chosen and be paid for. For instance, WindPRO can calculate noise generation caused by wind farms and a planner who works only with this issue only needs the DECIBEL (Noise) module. The software is available in many languages and is based on a user-friendly map and coordinate system, [5] [6].

The software can be used for various purposes such as:

- digitilising information on maps, such as height contours,

- simple energy estimations of single wind turbines and wind farms,

- calculate generation of noise and shadows,

- make photo montages of the landscape with wind turbines.

## 2.2 WAsP

WAsP, Wind Atlas Analysis and Application Program, is a wind simulation software based on a linear flow model. The software was initially developed in

the 80s Risø National Laboratory in Roskilde, Denmark, [12]. Risø National Laboratory merged with the Technical University of Denmark, DTU, in 2007 and is now known as Risø DTU National Laboratory for Sustainable Energy, [9]. WAsP is today developed and distributed by the wind energy division at Risø DTU and has more than 2900 users worldwide, [10].

WAsP can be used for various purposes such as:

- estimating and optimising wind farm production and efficiency,

- mapping of wind resources,

- digitilising information on maps, such as height contours.

## 2.3 WindSim

WindSim is a CFD wind simulation software based on a nonlinear flow model. The software was initially developed in the beginning of the 21st century by Vector AS in Tønsberg, Norway. In 1998 Vector AS conducted an inventory of the wind conditions along the complex coastline of Norway in cooperation with the Norwegian Meteorological institute and this was when the idea of WindSim was born. A UNIX beta version was launched in 2003 and the first commercial Windows based version was launched in 2005. This was also when the company changed its name from Vector AS to WindSim AS, [15]. Today WindSim has more than 150 licensed users, [17].

The software can be used for various purposes such as:

- estimating and optimising wind farm production and efficiency,

- mapping of wind resources.

The software is especially useful if the site has complex orography and/or complex climatology, [16].

# Chapter 3

# Flow models

## 3.1 Linear model

In this section the linear model used in WAsP will be presented. Originally, the WAsP model was described in Troen and Petersen (1989) and this section is based on this book, [12]. WAsP uses the wind atlas model which is a linear model combining a physical model (e.g. atmospheric stability, roughness changes, shelters and landscape orography) and a statistical model, i.e., Weibull distribution of the wind, in the analysis. For further details it is referred to Troen and Petersen (1989).

Equation 3.1 and 3.2 are used in WAsP in order to describe the surface layer wind profile. This is needed when transforming a wind speed at a certain height to a wind speed at another height.

$$u(z) = \frac{u_*}{\kappa} ln \frac{z}{z_0} \tag{3.1}$$

Where $u(z)$ is the air velocity at a height of $z$, $u_*$ is the air friction velocity, $\kappa$ is von Karmans constant which in this case is set equal to 0,40 and $z_0$ is the roughness length of the surface.

$$u(z) = \frac{u_*}{\kappa} \left( ln \frac{z}{z_0} - \psi(\frac{z}{L}) \right) \tag{3.2}$$

Equation 3.1 applies for high wind speeds over a homogenous terrain and is referred to as the logarithmic wind law, see figure 2.7. Equation 3.2 includes an empirical stability function, $\psi(\frac{z}{L})$, in order to compensate for lower wind speeds and surface heat flux. $L$ is the Monin-Obukhov length which is defined according to equation 3.3.

$$L = \frac{T_0}{\kappa g} \frac{c_p u_*^3}{H_0} \tag{3.3}$$

Where $T_0$ and $H_0$ are the absolute temperature and heat flux, respectively. $c_p$ is the heat capacity of air at constant pressure and $g$ is the gravitation constant.

The geostrophic wind is incorporated by WAsP in the geostrophic drag law, equation 3.4, which is a balance between the friction velocity and the geostrophic wind.

$$G = \frac{u_*}{\kappa} \sqrt{\left(ln(\frac{u_*}{f z_0}) - A(\mu)\right)^2 + B(\mu)^2} \tag{3.4}$$

A and B parameters are at neutral stability conditions constants but at non-neutral stability conditions they are function of $\mu$, the atmospheric stability parameter which is described in equation 3.5.

$$\mu = \frac{\kappa u_*}{f L} \tag{3.5}$$

### 3.1.1 Stability submodel

This model describes the stability of the atmosphere. It is derived from the geostrophic drag law and accounts for variations in surface heat flux which in turn will have an impact on the wind profile. Instead of treating each variation of the surface heat flux and its impact on the wind profile, the model uses the root-mean-square of the heat flux. Among other equations the empirical stability equation, equation 3.6, is derived and described for stable and unstable conditions.

$$\psi(\frac{z}{L}) = \begin{cases} -4.7\frac{z}{L} & \text{if conditions are stable} \\ \left(1 - 16\frac{z}{L}\right)^{1/4} - 1 & \text{if conditions are unstable} \end{cases} \tag{3.6}$$

### 3.1.2 Roughness change submodel

The logarithmic wind profile is valid only for homogenous terrain conditions. If the roughness of the terrain changes, the logarithmic wind profile has to be compensated in order to cover for these changes. When there is a change of roughness, the height of the internal boundary layer will change. The wind profile above the boundary layer before the change will be unaffected but the wind profile below will change, as shown in figure 3.1.
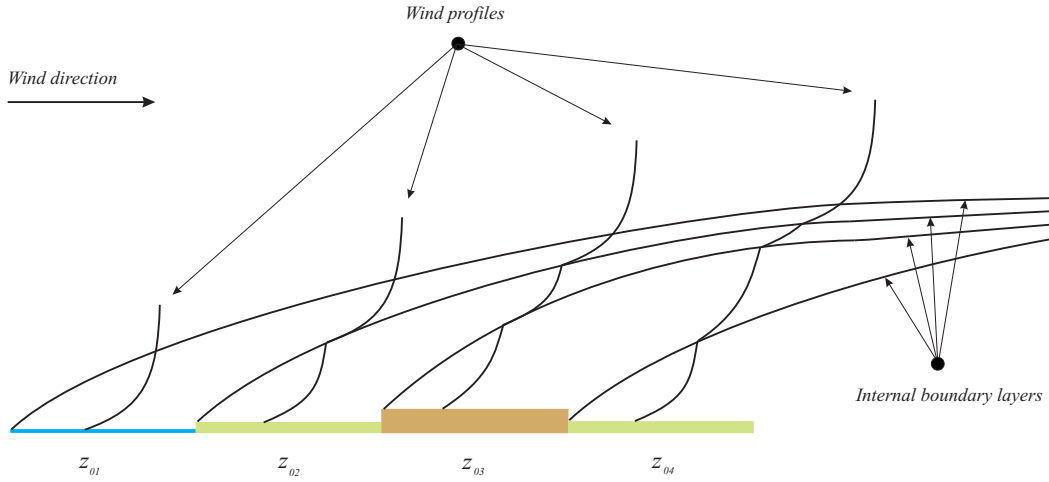


**Figure 3.1:** The change of wind profile due to roughness change.

Equation 3.7 has empirically been established between the friction velocity before, $u_{*1}$, and after, $u_{*2}$, the change and the roughness length before, $z_{01}$, and after, $z_{02}$ the change.

$$\frac{u_{*2}}{u_{*1}} = \frac{ln(h/z_{01})}{ln(h/z_{02})} \tag{3.7}$$

Where $h$ is the height of the internal boundary layer.

The perturbed wind profile is divided into three parts by the submodel and is described by equation 3.8.

$$u(z) = \begin{cases} u' \frac{ln(z/z_{01})}{ln(c_1 h/z_{01})} & \text{for } z \geq c_1 h \\ u'' + (u' - u'') \frac{ln(z/c_2 h)}{ln(c_1/c_2)} & \text{for } c_2 h \leq z \leq c_1 h \\ u'' \frac{ln(z/z_{02})}{ln(c_2 h/z_{02})} & \text{for } z \leq c_2 h \end{cases} \tag{3.8}$$

Where $u' = \frac{u_{*1}}{\kappa} ln \frac{c_1 h}{z_{01}}$, $u'' = \frac{u_{*2}}{\kappa} ln \frac{c_2 h}{z_{02}}$, $c_1 = 0.3$ and $c_2 = 0.09$.

### 3.1.3 Shelter submodel

The wind profile at the site of the turbine is affected by all obstacles close to the turbines. Obstacles in a general view are everything ranging from individual sand grains and leaves to large trees and buildings. Most of these obstacles are however already described by the roughness length and are not covered in the shelter model. The shelter model corrects the wind profile for deviations due to large single obstacles such as buildings. After the obstacle a wind wake will emerge. The size of the wake is mainly affected by the size and porosity of the obstacle. The wind wake leads to a decrease in wind speed behind the obstacle. The decrease is derived empirically and can be defined as equation 3.9.

$$\frac{\Delta u}{u} = 9.8 \left(\frac{z_a}{h}\right)^{0.14} \frac{x}{h}(1 - P_{eta})\eta exp(-0.67\eta^{1.5}) \tag{3.9}$$

Where $\frac{\Delta u}{u}$ describes the decrease in wind speed, $P_{eta}$ the porosity, $h$ the height of the obstacle, $z_a$ the considered height and $x$ the downstream distance. $\eta$ is defined according to equation 3.10.

$$\eta = \frac{z_a}{h} \left(\frac{0.32}{ln(h/z_0)} \frac{x}{h}\right)^{-0.47} \tag{3.10}$$

### 3.1.4 Orographic submodel

The orography model corrects the measured wind data to correspond to height variations around the wind mast and the wind turbine. The model uses a horizontal grid which expands radially from the site of the turbine and the wind measuring point and uses polar representation, as shown in figure 3.2. The resolution is higher closer to the points of interest and decreases with factor to 1.06 radially. This allows a very high resolution close to the point of interest.

Slopes and height variations however affect the logarithmic wind profile in such a way so that wind speed increases closer to the ground as presented in figure 3.3.
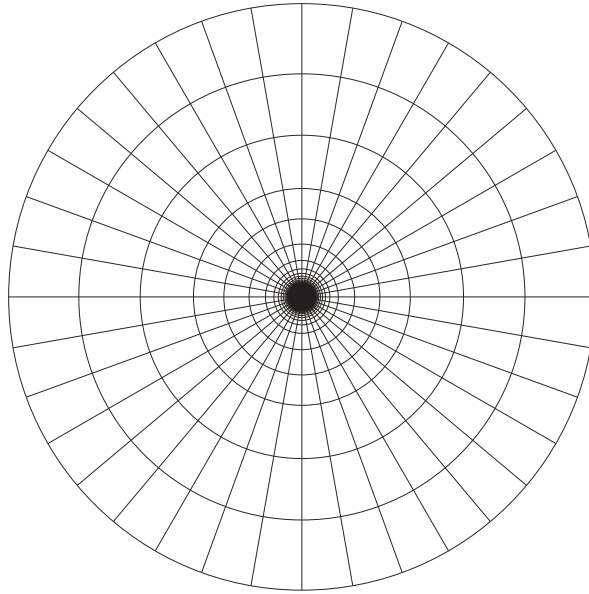
**Figure 3.2:** The radial grid.
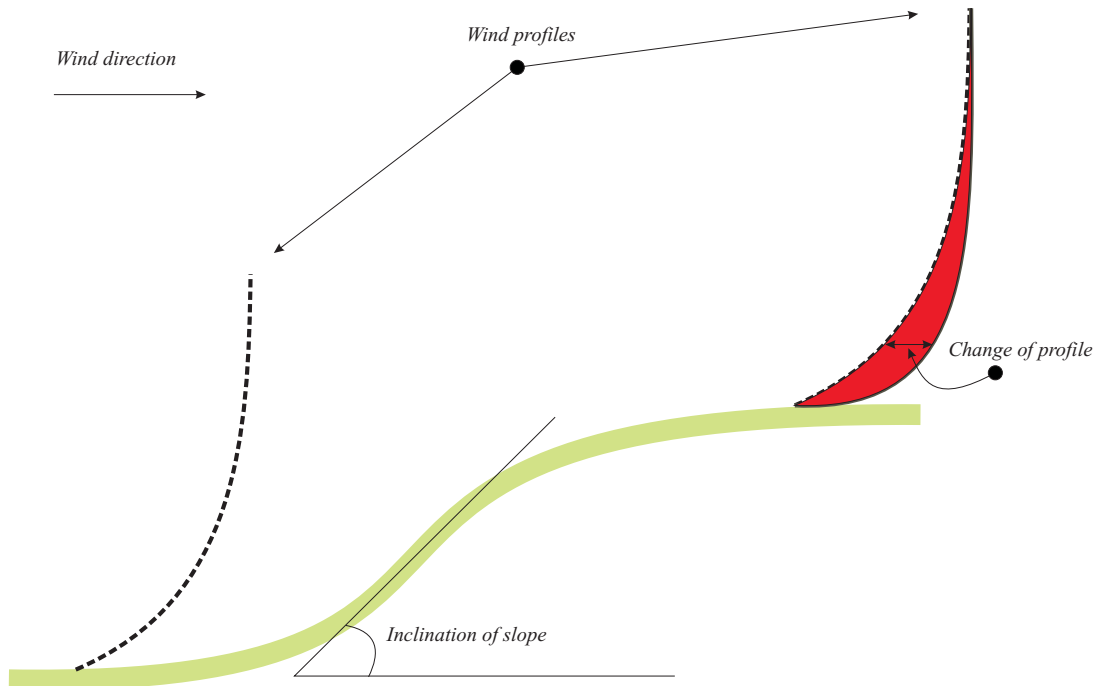


**Figure 3.3:** Change of the wind profile due to the slope.

## 3.2   Nonlinear flow models

This section will take a look of some common CFD methods. CFD simulations are based on the Navier-Stokes equations, which will be presented in a first step.

### 3.2.1   Navier-Stokes equations

The following three different Navier-Stokes equations describe the motion of fluids and are based on conservation of momentum, mass and energy.

**Mass conservation**   If we have a look on the mass conservation, one can determine that the same amount of mass that enters a control volume must leave the volume with the same rate. This leads to the mass conservation equation which is defined according to equation 3.11.

$$\frac{\partial \rho}{\partial t} + \frac{\partial (\rho u_i)}{\partial x_i} = 0 \tag{3.11}$$

Where $\rho$ is the density, $t$ is time, $u_i$ is the velocity vector and $x_i$ is the directional coordinate.

If the fluid is incompressible (such as water), or Newtonian incompressible (such as air) the density becomes independent of time and and space which leads to the mass conservation equation for incompressible flow:

$$\frac{\partial u_i}{\partial x_i} = 0 \tag{3.12}$$

**Momentum conservation**   This equation stems from the second law of Newton but also consist of a vicious stress term and a pressure term.

$$\frac{\partial u_i}{\partial t} + u_j \frac{u_i}{x_j} = -\frac{1}{\rho}\frac{\partial p}{\partial x_i} + \frac{\partial}{\partial x_j}\left[\nu\left(\frac{\partial u_i}{\partial x_j} + \frac{\partial u_j}{\partial x_i}\right)\right] + f_{body,i} \tag{3.13}$$

For steady state incompressible flow this equations becomes as equation 3.14 (combination of equation 3.12 and 3.13).

$$\frac{\partial u_i}{\partial t} + u_j \frac{u_i}{x_j} = -\frac{1}{\rho}\frac{\partial p}{\partial x_i} + \nu\frac{\partial^2 u_i}{\partial x_j^2} + f_{body,i} \tag{3.14}$$

**Energy conservation**   Since we treat the temperature as constant and that air is Newtonian incompressible, the energy equation is decoupled. The equation is not interesting when determining flows unless one would like to look at heat transfer issues.

NOTE, The energy equation has NOTHING to do with the energy production of a wind turbine/farm.

**Using the full Navier-Stokes equations**   Resolving the Navier-Stokes equations as they are defined above requires immense computer power. This is generally done by using DNS (Direct Numerical Simulation) where simulations are executed on small models of e.g. air foils. If the models become larger, simplifications of the Navier-Stokes equations are necessary due to computer power limitations.

## 3.2.2   Simplifications used in WindSim code

WindSim uses a so called RANS model in the calculation. RANS stands for Reynold's Averaged Navier-Stokes and is basically the Navier-Stokes equations averaged over time. The mass conservation equation has no time dependency in the incompressible form, and remains as for the full equation. However, the momentum equation is defined accordning to equation 3.15 in which ime dependencies are removed and some extra terms are added.

$$u_j \frac{u_i}{x_j} = -\frac{1}{\rho}\frac{\partial p}{\partial x_i} + \frac{\partial}{\partial x_j}\left[\nu\left(\frac{\partial u_i}{\partial x_j} + \frac{\partial u_j}{\partial x_i}\right) - \overline{u_i u_j}\right] + f_{body,i} \qquad (3.15)$$

Which in its rewritten form becomes as equation 3.16

$$u_j \frac{u_i}{x_j} = -\frac{1}{\rho}\frac{\partial p}{\partial x_i} + \frac{\partial}{\partial x_j}\left[(\nu + \nu_T)\left(\frac{\partial u_i}{\partial x_j} + \frac{\partial u_j}{\partial x_i}\right) - \frac{2}{3}k\delta_{ij}\right] + f_{body,i} \qquad (3.16)$$

$$\nu_T = c_\mu \frac{k^2}{\varepsilon} \qquad (3.17)$$

Where $c_\mu$ is a model constant, $k$ is the turbulent kinetic energy and $\varepsilon$ is the turbulence dissipation rate.

**Turbulence model**   Turbulence, i.e., fast fluctuations in wind speeds and directions, occurs in most applications and is therefore important to implement in the calculations. When using a DNS model, one uses the full

Navier-Stokes equations which can account for turbulence, i.e., nonlinear effects, directly since the number of equations matches the number of unknown variables (flow variables). However, when using simplified sets of the Navier-Stokes equations it requires some kind of turbulence model in order to solve the equations. The simplification produces some extra terms in the Navier-Stokes equation and without the turbulence model the number of equations would be to low compared to the number of flow variables. In the WindSim interface, one can choose from different turbulence models. The default, i.e., the standard $k - \varepsilon$ model is described below.

Equation 3.18 and 3.19 describe the transport equations for $k$ and $\varepsilon$.

$$\frac{Dk}{Dt} = \frac{\partial}{\partial x_i} \left[ \left( \nu + \frac{\nu_T}{\sigma_k} \right) \frac{\partial k}{\partial x_i} \right] + P_k - \varepsilon \tag{3.18}$$

$$\frac{D\varepsilon}{Dt} = \frac{\partial}{\partial x_i} \left[ \left( \nu + \frac{\nu_T}{\sigma_\varepsilon} \right) \frac{\partial \varepsilon}{\partial x_i} \right] + c_{\varepsilon 1} \frac{\varepsilon}{k} P_k - c_{\varepsilon 2} \frac{\varepsilon^2}{k} \tag{3.19}$$

Where the turbulent production term, $P_k$ is described according to equation 3.20

$$P_k = \nu_T \left( \frac{\partial u_i}{\partial x_j} + \frac{\partial u_j}{\partial x_i} \right) \frac{\partial u_i}{\partial x_j} \tag{3.20}$$

### 3.2.3   Discretization

The Navier-Stokes equations are basically continious differential equations. In order to make them suitable for numerical computing, such as CFD calculations, one uses discretization, which implements a transformation of the Navier-Stokes equation into discrete difference equations. The idea of discretization is shown below for a heat transfer in a stick.

$$\frac{\partial u}{\partial t} = \alpha \frac{\partial^2 u}{\partial x^2} \tag{3.21}$$

$$0 \leq x \leq L$$
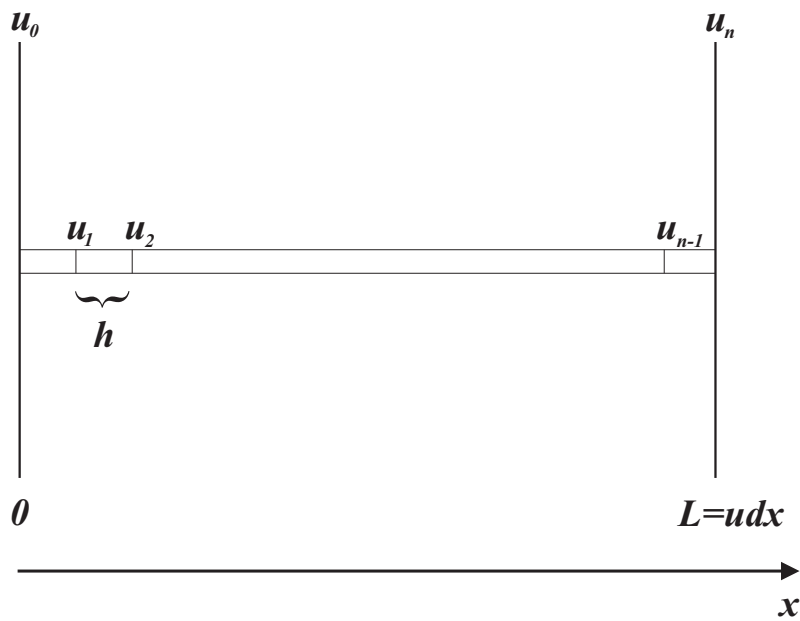
Boundnary conditions (B.C.):

$x = 0$ :

$$cu + \frac{\partial u}{\partial x} = sint \implies u_0(t) = \frac{sint - \frac{\partial u}{\partial x}}{c} \qquad (3.22)$$

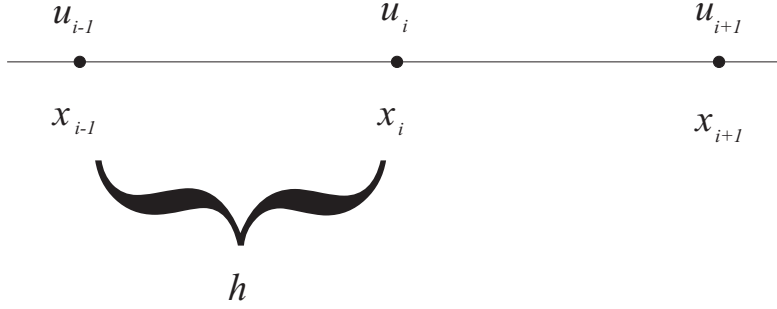$x = L$ :

$$u_n(t) = 0 \qquad (3.23)$$

Furthermore,



$$\frac{d\overline{u}}{dt} = A\overline{u} + \overline{h} \qquad (3.24)$$

where,

$$\overline{u} = (u_1, u_2, ..., u_n)^T \qquad (3.25)$$

which gives,

$$i = (0, 1, 2, ...., n) \qquad (3.26)$$

which gives,

$$\frac{\partial u}{\partial x} = \frac{u_{i+1} - u_{u+1}}{2h} \tag{3.27}$$

and

$$\frac{\partial^2 u}{\partial x^2} = \frac{\frac{u_{i+1} - u_i}{h} - \frac{u_i - u_{i-1}}{h}}{2h} = \frac{u_{i+1} - 2u_i + u_{i-1}}{2h^2} \tag{3.28}$$

When $i = 0$:

$$cu_0 + \frac{u_1 - u_{-1}}{2h} = sint \implies u_{-1} = 2hu_0 c - 2h sint + u_1 \tag{3.29}$$

Furthermore,

$$\frac{du_0}{dt} = \frac{\alpha}{2h^2}[u_1 - 2u_0 + u_{-1}] = \frac{\alpha}{2h^2}[u_1 - 2u_0 + 2hu_0 c - 2h sint + u_1] \tag{3.30}$$

$$= \frac{\alpha}{h^2}\left[(hc - 1)u_0 + u_1) - \frac{\alpha}{h} sint\right]$$

When $i = 1$:

$$\frac{du_1}{dt} = \frac{\alpha}{h^2}(\frac{1}{2}u_2 - u_1 + \frac{1}{2}u_0) \tag{3.31}$$

$i = 2$:

$$\frac{du_2}{dt} = \frac{\alpha}{h^2}(\frac{1}{2}u_3 - u_2 + \frac{1}{2}u_1) \tag{3.32}$$

When $i = n - 1$:

$$\frac{du_{n-1}}{dt} = \frac{\alpha}{h^2}(\frac{1}{2}u_n - u_{n-1} + \frac{1}{2}u_{n-2})$$
(3.33)

Further, all $\frac{du}{dt}$ are put together in the matrix $\frac{d\overline{u}}{dt}$.

$$\frac{d\overline{u}}{dt} = \frac{\alpha}{h^2}
\begin{bmatrix}
hc-1 & 1 & 0 & 0 & . & . & . & . & . & 0 \\
\frac{1}{2} & -1 & \frac{1}{2} & 0 & & & & & & \\
0 & \frac{1}{2} & -1 & \frac{1}{2} & & & & & & \\
. & & & & & & & & & \\
. & & & & & & & & & \\
. & & & & & & & & & \\
0 & . & . & . & . & . & . & \frac{1}{2} & -1 & \frac{1}{2}
\end{bmatrix}
\begin{bmatrix}
u_0 \\ u_1 \\ u_2 \\ u_3 \\ . \\ . \\ . \\ . \\ . \\ u_{n-2} \\ u_{n-1} \\ u_n
\end{bmatrix}
+ \frac{\alpha}{h}
\begin{bmatrix}
-sint \\ 0 \\ . \\ . \\ . \\ .
\end{bmatrix}$$

## 3.2.4  Calculation process

Since the Navier-Stokes equations are nonlinear differential equations there are no analytical solutions to them hence the calculations are iterative. This requires some sort of initial values of the flow variables. The initial values of the flow variables in WindSim for the standard $k - \varepsilon$ turbulence model are:

$$u(z) = \frac{u_*}{\kappa}ln\frac{z}{z_0}$$
(3.34)

$$k = \frac{u_*^2}{\sqrt{c_\mu}}$$
(3.35)

$$\varepsilon = \frac{u_*^3}{\kappa d}$$
(3.36)

The usage of such pregenerated values and profiles will in most cases in turn generate a fault close to the inlet (close to the boundaries). Points of interests should therefore not be situated close to the borders of the domain.

For more information regarding the specific WindSim equations it is refered to Gravdahl and the insoftware Wiki.

## 3.3 Differences

Imagine a wind measuring device placed on top of a hill. If the hill slope is less than approximately 17° or 30%, the wind will accelerate up the hill and the measuring device on the hill will register a high wind speed. If the slope is larger than 17°, wind separation occurs, as shown in figure 3.4, and the registered wind speed is low. The major difference between the two software and their models in this aspects is how they treat this separation.
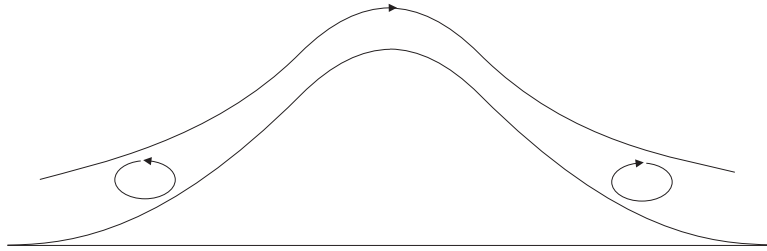


**Figure 3.4:** Wind separation due to high angle slope, [14].
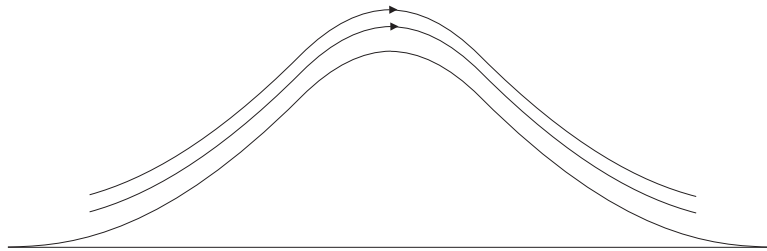


**Figure 3.5:** The attached wind in linear model, [14].

The linear model used in WAsP cannot account for this separation and treats the flow as attached over the hill, as shown in figure 3.5. This basically leads to an overestimation of wind speed prediction for hills with a larger slope than 17°.

The nonlinear model used in WindSim can however account for this separation due to the use of the turbulence model. The accuracy of the wind speed prediction is therefore high even for slopes that exceed 17°, [14].

Energy is proportional to the wind speed to the power of three, equation 3.37.

$$E_{kin} = ku^3 \qquad (3.37)$$

The energy for the wind speed of 10 m/s is determined by equation 3.38.

$$E_{kin}(u = 10) = k10^3 = k1000 \tag{3.38}$$

If the wind speed is predicted as 10% too high, i.e., totally 11 m/s, the energy is determined by equation 3.39.

$$E_{kin}(u = 11) = k11^3 = k1331 \tag{3.39}$$

The percental increase of energy due to the over estimation of wind speed is described in equation 3.40

$$\frac{E_{kin}(u = 11) - E_{kin}(u = 10)}{E_{kin}(u = 10)} * 100 = 33,1\% \tag{3.40}$$

Figure 3.6 shows the simulation outcome difference for two real cases executed parallel in WAsP and WindSim in comparison with measured data. The Siral simulation is executed at a site with low orographic complexity, Näsudden and the Ferdinand, Vilhelm and Freja simulations are executed at a site with high orographic complexity, Hunnflen. In the low complexity case the simulated energy production in both WAsP and WindSim is almost identical to the measured production. For the high complexity cases the WindSim simulated production is very close to the measured production while the WAsP simulated energy production is clearly overestimated.
.
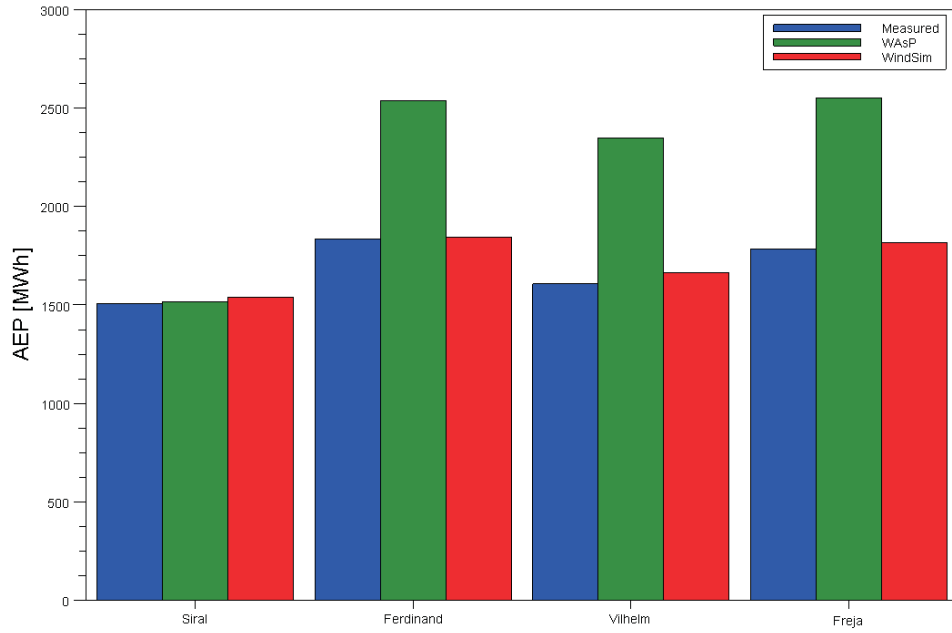
**Figure 3.6:** Measured and estimated energy production.

# Bibliography

[1] S. A. Ackerman and J. A. Know. *Meteorology: Understanding the Atmosphere*. Thomson Brooks/Cole, Pacific Grove, CA, 2003.

[2] D. C. Ahrens. *Meteorology today: an introduction to weather climate and the environment*. Cengage Learning, Minneapolis, 2007.

[3] H. Bergstrom. Vindkartering. http://www.energimyndigheten.se/. Accessed: 2010-04-01.

[4] J. Bogren. *Klimatologi, meteorologi*. Studentlitteratur, Lund, 1999.

[5] EMD. EMD. http://emd.dk. Accessed: 2010-01-01.

[6] EMD. WindPRO. http://emd.dk/windpro/. Accessed: 2010-01-01.

[7] S. Ivanell. *Numerical Computations of Wind Turbine Wakes*. KTH Engineering Sciences, Stockholm, 2009, ISBN 978-91-7415-216-6.

[8] N. O. Jensen. *A Note on Wind Generator Interaction*. Risø National Laboratory, Roskilde, 1983.

[9] Risø. Facts about Risø. http://www.risoe.dk/. Accessed: 2009-12-01.

[10] Risø. WAsP. http://www.wasp.dk/. Accessed: 2009-12-01.

[11] R. B. Stull. *An Introduction to Boundary Layer Meteorology*. Kluwer Academic Publishers, Vancouver, 1988.

[12] I. Troen and E. L. Petersen. *European Wind Atlas*. Risø National Laboratory, Roskilde, 1989.

[13] Vindmolleindustrien. Power Control of Wind Turbines. http://guidedtour.windpower.org/. Accessed: 2010-01-01.

[14] T. Wallbank. Windsim validation study: CFD validation in complex terrain. Documentation for WindSim users, 2008.

[15] WindSim. History. http://www.windsim.com/. Accessed: 2009-12-01.

[16] WindSim. Product overview. http://www.windsim.com/. Accessed: 2009-12-01.

[17] WindSim. WindSim: The Basics. Documentation for WindSim users, 2009.

[18] T. Wizelius. *Vindkraft i teori och praktik*. Studentlitteratur, Lund, 2007.